Journal of Alloys and Compounds 509 (2011) 2567–2571

Contents lists available at ScienceDirect

Journal of Alloys and Compounds

journal homepage: www.elsevier.com/locate/jallcom

Chemical synthesis of Fe_2O_3 thin films for supercapacitor application

P.M. Kulal, D.P. Dubal, C.D. Lokhande, V.J. Fulari *

Holography and Material Research Laboratory, Department of Physics, Shivaji University, Kolhapur 416004, M.S., India

ARTICLE INFO

Article history:
Received 30 September 2010
Received in revised form
10 November 2010
Accepted 11 November 2010
Available online 19 November 2010

Keywords:
SILAR
Iron oxide
Microstructure
Supercapacitor

ABSTRACT

Fe_2O_3 thin films have been prepared by novel chemical successive ionic layer adsorption and reaction (SILAR) method. Further these films were characterized for their structural, morphological and optical properties by means of X-ray diffraction (XRD), Fourier transform infrared (FTIR) spectrum, scanning electron microscopy (SEM), wettability test and optical absorption studies. The XRD pattern showed that the Fe_2O_3 films exhibit amorphous in nature. Formation of iron oxide compound was confirmed from FTIR studies. The optical absorption showed existence of direct optical band gap of energy 2.2 eV. Fe_2O_3 film surface showed superhydrophilic nature with water contact angle less than 10°. The supercapacitive properties of Fe_2O_3 thin film investigated in 1 M NaOH electrolyte showed supercapacitance of 178 F g^{-1} at scan rate 5 mV/s.

1. Introduction

In recent years, growing demands for power sources of transient high-power density have stimulated a great interest in electrochemical supercapacitor with project applications in digital communications, electric vehicles, burst power generation, memory back-up devices and other related devices which require high-power pulses. The potential applications of electrochemical capacitors include the power enhancement and cycle life improvement of primary power sources such as batteries and fuel cells. Electrochemical capacitors are also attractive for other applications such as power sources for camera flash equipment, lasers, and cellular phones. Electrochemical supercapacitors are divided into two categories according to different energy-storage mechanisms (i) redox supercapacitors, in which the pseudocapacitance arises from faradic reactions occurring at the electrode interface and (ii) electric double layer capacitors (EDLCs), in which the capacitance arises from the charge separation at the electrode/electrolyte interface. The main materials that have been studied for the supercapacitor electrode are (i) carbons, (ii) transition metal oxides and (iii) conducting polymers [1].

Various transition-metal oxides, such as RuO_2, Co_3O_4, NiO, Fe_2O_3, IrO_2, SnO_2, MnO_2, etc., are being studied for the supercapacitor applications. Among these metal oxides for supercapacitor electrodes, amorphous hydrous RuO_2 is the most promising material for supercapacitors because of its high specific capacitance, excellent reversibility, and long cycle life. However, RuO_2 is expensive, toxic, and naturally less abundant, which limits their commercial use. Accordingly, there is a strong incentive to find alternative electrode materials, which are inexpensive and exhibit pseudocapacitance similar to that of amorphous $RuO_2 \cdot xH_2O$. To this end, much attention is now focused on the oxides of manganese [2], nickel [3], cobalt [4], vanadium [5] and copper [6] as candidate for electrode materials.

Alternately we propose the iron oxide, the transition material having low cost for use in supercapacitor. Iron oxide thin films have been prepared by various methods, such as the sol–gel [7], chemical vapor deposition [8] and electrodeposition [9], spray pyrolysis [10]. Among these chemical methods, successive ionic layer absorption and reaction (SILAR) is low cost and low temperature soft chemical solution method. The SILAR method is relatively a new and less investigated method, which is based on sequential reaction on the substrate surface. Rinsing follows each reaction, which enables heterogeneous reaction between the solid phase and the solvated ions in the solution. SILAR method has its own advantages such as layer-by-layer growing mode, excellent material utilization efficiency, and good control over the deposition process along with the film thickness and large-scale deposition capability on any type of substrate [11].

In the present investigation, we first time report the synthesis of Fe_2O_3 thin films by SILAR method. These films were characterized by XRD, FTIR, SEM, wettability test and optical absorbance studies. The supercapacitive behavior of Fe_2O_3 thin film was investigated by cyclic voltammetry in 1 M NaOH electrolyte. The effect of scan rate on the supercapacitance of Fe_2O_3 thin film has been investigated.

* Corresponding author. Tel.: +91 231 2609224; fax: +91 231 2692333.
E-mail address: vijayfulari@gmail.com (V.J. Fulari).

0925-8388/$ – see front matter © 2010 Elsevier B.V. All rights reserved.
doi:10.1016/j.jallcom.2010.11.091

2. Experimental

2.1. Synthesis of Fe_2O_3 thin films

For the deposition of Fe_2O_3 thin films, 0.05 M ferrous sulphate was used as the cationic precursor solution and anionic precursor solution was 0.1 M sodium hydroxide. The well cleaned glass/stainless steel (SS) substrate was immersed in a cationic precursor solution ($FeSO_4$) for 10 s for the adsorption of iron species on the substrate surface. The substrate was rinsed in double distilled water for 5 s to remove loosely bound species of Fe^{2+} species. Then, the substrate was immersed in anionic precursor solution (NaOH) which was kept at 333 K for 15 s to form a layer of iron oxide material. Rinsing the substrate again in double distilled water for 5 s separates out the excess or unreacted species. Thus one SILAR cycle of Fe_2O_3 deposition was completed. 120 such deposition cycles were repeated at room temperature (300 K) to get a terminal thickness. The maximum thickness obtained for Fe_2O_3 thin film was 1.2 μm and used for the further.

2.2. Characterization techniques

For thickness measurement, gravimetric weight difference method with the relation $t = m/(\rho \times A)$ where m is the mass of the film deposited on the substrate in gm; A is the area of the deposited film in cm^2 and ρ is the density of the deposited material (Fe_2O_3 = 5.242 g cm^{-3}) in bulk form. The crystal structure of the film material was identified by X-ray diffraction analysis with Philips (PW 3710) diffractometer. The Fourier transform infrared (FTIR) spectrum of the samples was collected using a 'Perkin Elmer, FTIR Spectrum one' unit. The film morphology was observed by scanning electron microscopy (Model: JEOL 6360). To study the wettability of the films, contact angle measurement was carried out by Rame-hart USA equipment with CCD camera. The optical absorption studies were carried out within the wavelength range 350–850 nm for Fe_2O_3 films using Systronics spectrophotometer-119, with glass substrate as reference. The supercapacitor formation and its studies were carried out using the 263A EG &G Princeton Applied Research Potentiostat forming an electrochemical cell comprising Fe_2O_3 film as a working electrode, platinum as a counter electrode and saturated calomel electrode (SCE) as a reference electrode in 1 M NaOH electrolyte.

3. Results and discussion

3.1. Film formation mechanism

Fe_2O_3 thin films were prepared by immersing substrate in separately placed cationic and anionic precursors with rinsing between every immersion. The growth kinetics of a thin film deposition process is ion-by-ion growth mechanism, which involves the ion-by-ion deposition at nucleation sites on the immersed surfaces. The mechanism of Fe_2O_3 film formation by SILAR method is explained as follows. The hydrolysis of ferrous sulphate takes place with pH ~5 which gives ferrous hydroxyl $Fe(OH)_2$ ions.

$$FeSO_4 + 2NaOH \rightarrow Fe(OH)_2 + Na_2SO_4 \quad (1)$$

When substrate is immersed in this solution, $Fe(OH)_2$ ions get adsorbed onto the substrate due to attraction between ions in the solution and surface of the substrate. These forces may be cohesive forces or van der Waals forces or chemical attractive forces. Further reaction is followed by the immersion of substrate in NaOH anionic solution, where the chemical reaction between OH^- and $Fe(OH)_2$ ions leads to the deposition of adherent Fe_2O_3 layer.

$$2Fe(OH)_2 + 2OH^- \rightarrow Fe_2O_3 + 3H_2O \quad (2)$$

Fe_2O_3 thin films are uniform and well adherent to the substrate surface. Here, for the deposition of Fe_2O_3 thin films the adsorption period was 10 s and reaction period was 15 s. The optimized preparative parameters are summarized in Table 1.

3.2. Thickness measurement

Thickness of Fe_2O_3 films was measured by the gravimetric weight difference method in terms of deposited weight of a Fe_2O_3 film on the glass substrate, per unit area (g cm^{-2}), since the accurate measurement of Fe_2O_3 film thickness was not possible due to the rough morphology and porosity of the film. The graph of the deposited weight of Fe_2O_3 with the number of cycles is shown in Fig. 1. In the process of deposition of Fe_2O_3 films by SILAR method, Fe_2O_3 thin films were prepared by immersing substrate in separately placed cationic and anionic precursors with rinsing between every immersion. The weight of Fe_2O_3 film was found to increase with number of cycles. After 120 cycles, the thickness of the film decreases. The thickness of Fe_2O_3 thin films is 0.74, 0.91, 1.2 μm at 40, 80 and 120 cycles, respectively. The maximum thickness obtained for Fe_2O_3 thin film was 1.2 μm and used for the further characterization.

Table 1
Optimized preparative parameters for deposition of Fe_2O_3 thin films.

Precursors	$FeSO_4$	NaOH
Concentrations	0.05 M	0.1 M
Immersion time	10 s	10 s
Number of immersions	120	120
Thickness (μm)	1.20	–
Deposition temperature	300 K	343 K

3.3. Structural studies

Iron oxides crystallize in several different structures with varied proportions of Fe ions (Fe^{2+} and Fe^{3+}). The stable and well-known structures of iron oxides are FeO, Fe_2O_3 and Fe_3O_4. From these structures, Fe_2O_3 is normal spinel oxide which is room temperature stable structure with Fe^{2+} in the octahedral positions and Fe^{3+} in the tetrahedral positions of the spinel structure. Fig. 2 shows the XRD patterns of Fe_2O_3 thin films on to glass substrate. From XRD pattern it is seen that there is no peak corresponding to Fe_2O_3 material. This indicates the formation of amorphous material on the substrate. Amorphous phase of the material is feasible for supercapacitor application due to easy penetration of ions through the bulk of the active material [12].

3.4. FTIR studies

In order to know the chemical bonds present in the Fe_2O_3 compound, the sample was characterized by FTIR within the wavelength range 450–4000 cm^{-1}. Fig. 3 displays the FTIR spectrum of Fe_2O_3 sample. The sample shows the absorption in the region 3416, 1026, 605 and 465 cm^{-1}. The absorption at 3416 cm^{-1} indicates the presence of hydroxide group [13]. The absorption peaks around at 1611 and 1026 cm^{-1} may be attributed to O–H bending vibrations combined with Fe atoms. The peaks at 605 and 465 cm^{-1} correspond to the metal–oxygen (Fe–O) vibrational modes of the spinel compound, also these two peaks are characteristics of spinel com-

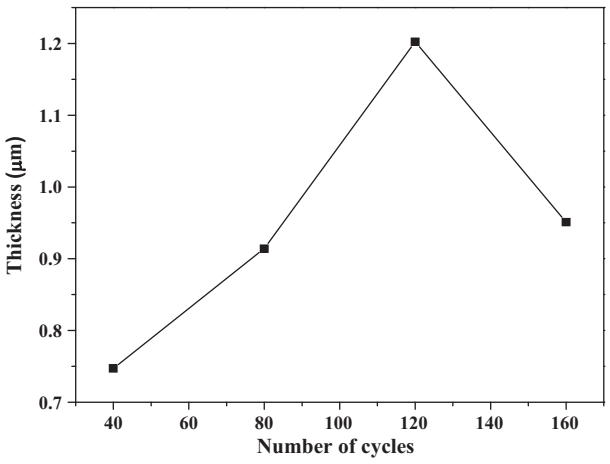

Fig. 1. Variation of Fe_2O_3 film thickness with number of cycles.

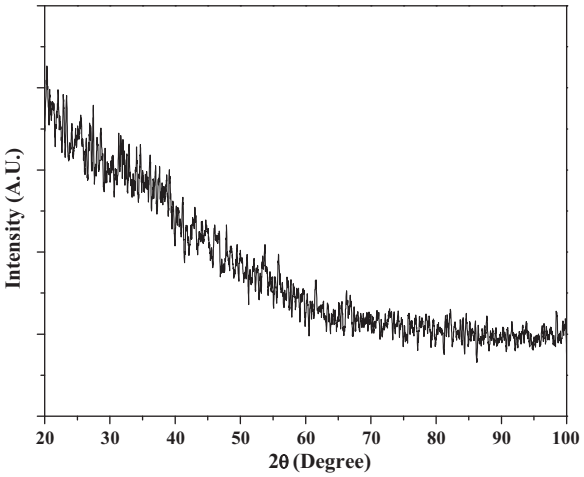

Fig. 2. XRD pattern of Fe_2O_3 thin film on to glass substrate.

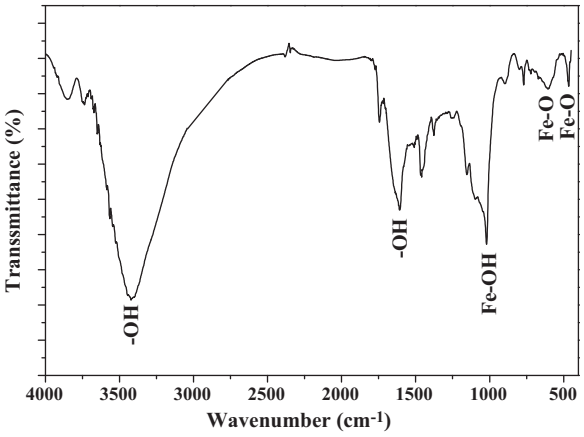

Fig. 3. FTIR spectrum of Fe_2O_3 compound.

pounds. These two bands are sharp and are of small intensity Fe–O peaks which is in good agreement with the literature [11]. Result indicates the presence of Fe–O bonds, and –OH groups for Fe_2O_3 thin films. Thus the formation of Fe_2O_3 compound is confirmed.

3.5. Surface morphology

Fig. 4 shows SEM images of Fe_2O_3 thin films at two different magnifications (×5000 and ×10,000). From SEM image (Fig. 4), it is seen that Fe_2O_3 film surface is porous and well covered with smooth, irregular shaped grains of random size. We clearly observed the grains which are interconnected with each other. These interconnected grains form clusters with some clusters of overgrowth. Such overgrowth can be explained on the basis of nucleation and coalescence process. Initially grown nano grains may have increased their size by further deposition and come closer to each other. Thus, the larger grains appear to grow by coalescence of smaller ones. The grains were small with non-uniform and no well-defined grain boundaries; hence it was difficult to calculate the exact average value of grain size. Such surface morphology with nanosized grains may offer increased surface area feasible for supercapacitor application [14].

Fig. 5. Water contact angle measurement of Fe_2O_3 thin film.

3.6. Wettability test

Wettability test is carried out in order to investigate the interaction between liquid and Fe_2O_3 thin films. If the wettability is high, contact angle (θ), will be small and the surface is hydrophilic. On the contrary, if the wettability is low, θ will be large and the surface is hydrophobic. A contact angle of 0° means complete wetting and a contact angle of 180° corresponds to complete non-wetting. Both super-hydrophilic and super-hydrophobic surfaces are important for practical applications [15]. From Fig. 5 we observed that, the Fe_2O_3 thin films are superhydrophilic as water contact angle is less than 10° means high wettability. This may be due to the strong cohesive force between the water droplet and hydroxide present in the iron oxide compound. Due to which the water is attracted rather repelled by the Fe_2O_3 film. This specific property is useful for making intimate contact of aqueous electrolyte with electrode surface in supercapacitor application. We believed

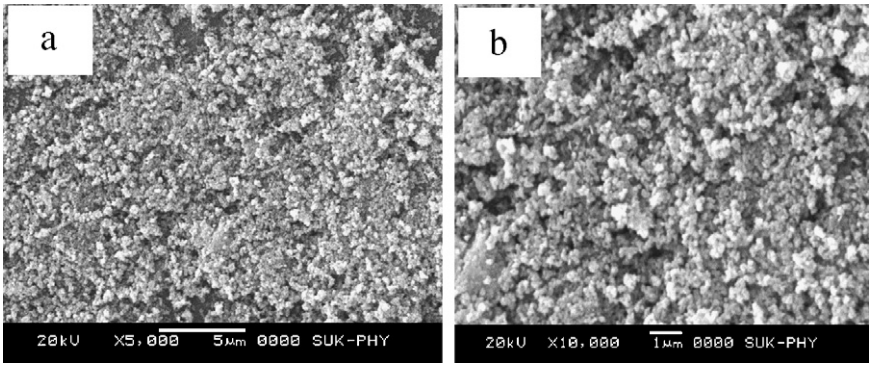

Fig. 4. SEM micrographs of Fe_2O_3 thin films at two different magnifications (a) ×5000 and (b) ×10,000.

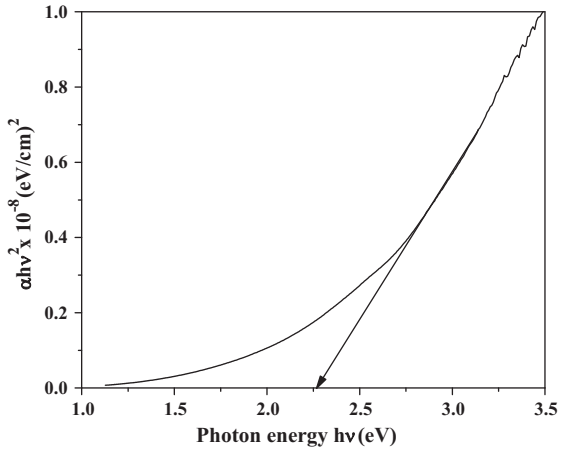

Fig. 6. Plot of $(\alpha h\nu)^2$ vs. photon energy $h\nu$ of Fe_2O_3 film.

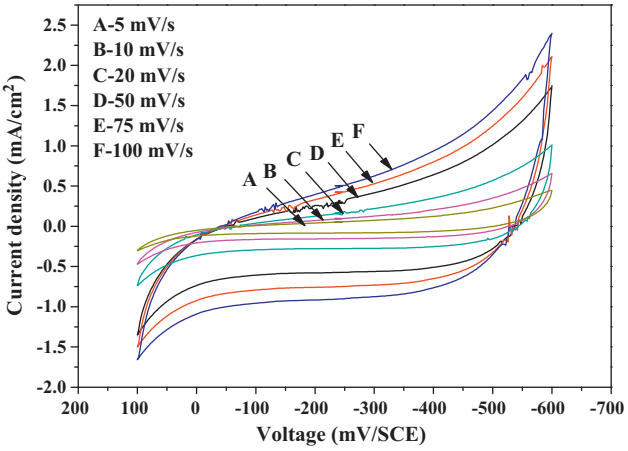

Fig. 7. The cyclic voltammograms of Mn_3O_4 thin film electrode at different scanning rates ((A) 5 mV/s, (B) 10 mV/s, (C) 20 mV/s, (D) 50 mV/s and (E) 100 mV/s) in the 1 M NaOH electrolyte in the working potential window of −0.6 to +0.1 V (vs. SCE).

this specific property will tentatively demonstrate the feasibility of Fe_2O_3 film surface useful in electrolyte/electrode interface for better performances. It is well known that in the electrochemical supercapacitor, hydrophilic surface of the electrode is an essential factor for better performance [16]. Mane et al. [17] reported a contact angle of 21° for electrochemically deposited tin oxide thin films for supercapacitor application.

3.7. Optical absorption study

The optical absorption spectrum of Fe_2O_3 thin film in the wavelength range 350–850 nm has been investigated. Fig. 6 shows the variation of $(\alpha h\nu)^2$ vs. $h\nu$ which is a straight line in the domain of higher energies, indicating a direct optical transition. The optical band gap of the Fe_2O_3 thin film is in good agreement with the literature data [18]. The theory of optical absorption gives the relationship between the absorption coefficients α and the photon energy $(h\nu)$,

$$\alpha = \frac{A(\mathrm{Eg} - h\nu)^n}{h\nu} \tag{3}$$

where A and ν are constants, for direct allowed transition $n = 1/2$ and for allowed indirect transition $n = 2$. The above Eq. (3) gives the band gap (Eg) when straight portion of $(\alpha h\nu)^2$ against $h\nu$ plot is extrapolated to the point $\alpha = 0$. From the graph, for Fe_2O_3 thin film the band gap value of 2.2 eV was obtained.

3.8. Supercapacitive studies

The chemically deposited amorphous Fe_2O_3 electrodes were used in the supercapacitor and their performances were tested using cyclic voltammogram (CV) technique. For finding the suitable electrolyte, the cyclic voltammograms of the Fe_2O_3 electrode in the 1.0 M NaOH aqueous electrolytes in the voltage range of −0.6 to +0.1 V/SCE were studied. In these cases, the Fe_2O_3 electrode exhibited symmetric CV characteristics in forward and reverse sweeps.

3.8.1. Cyclic voltammograms of Fe_2O_3 electrode

The chemically deposited Fe_2O_3 thin films were used in the formation of electrochemical supercapacitors and their performance was tested studying CV curves. Fig. 7 shows the CV curves of Fe_2O_3 electrode with different scan rates in 1 M NaOH electrolyte. It was found that the current under curve was slowly increased with scan rate. This shows that the voltammetric currents are directly proportional to the scan rates of CV, indicating an ideally capacitive behavior [12]. The capacitance (C) was calculated using following relation,

$$C = \frac{I_{\max}}{dv/dt} \tag{4}$$

where I is the average current in ampere and dv/dt is the voltage scanning rate. The interfacial capacitance was calculated using the relation,

$$C_i = \frac{C}{A} \tag{5}$$

where 'A' is the area of active material dipped in the electrolyte. The specific capacitance C_S ($\mathrm{F\,g^{-1}}$) of Fe_2O_3 electrode was calculated using following relation:

$$C_S = \frac{C_i}{W} \tag{6}$$

where W is the weight of Fe_2O_3 film dipped in electrolyte. The Fe_2O_3 electrode exhibited the interfacial capacitance of $0.12\,\mathrm{F\,cm^{-2}}$ and the supercapacitance of $178\,\mathrm{F\,g^{-1}}$. The large value in this case is attributed to the amorphous and porous nature of Fe_2O_3 thin films.

3.8.2. Effect of scan rate

The high or pulse-power property of Fe_2O_3 electrode is examined using cyclic voltammetry at different scan rates. Fig. 8 shows the CV curves of Fe_2O_3 electrode in 1 M NaOH electrolyte for different scan rates within voltage range of −0.6 to +0.1 V. Fig. 8 shows the variation of specific capacitance and interfacial capacitance with scan rate. From Fig. 8 it is seen that, specific and interfacial capacitance values are decreased from 178 to $121\,\mathrm{F\,g^{-1}}$ and 0.12

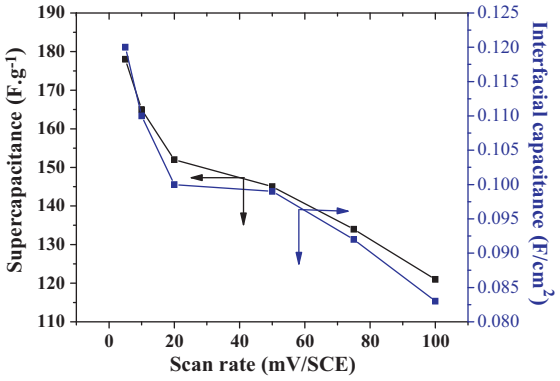

Fig. 8. Variation of specific and interfacial capacitances of Fe_2O_3 electrode at different scan rates. Concentration of NaOH electrolyte was 1.0 M.

to 0.089 F cm^{-2}, respectively. The maximum specific capacitance of 178 F g^{-1} was obtained at 5 mV/s. The decrease in capacitance has been attributed to the presence of inner active sites that cannot sustain the redox transitions completely at higher scan rates. This is probably due to the diffusion effect of protons within the electrode. The decreasing trend of the capacitance suggests that parts of the surface of the electrode are inaccessible at high charging–discharging rates [19]. Nagarajan and Zhitomirsky [9] prepared γ-Fe_2O_3 thin films by cathodic electrodeposition method and reported supercapacitance of 210 F g^{-1} in 0.25 M $Na_2S_2O_3$ electrolyte. Brousse and Belanger [20] prepared Fe_3O_4 powders with high surface area and reported a SC of 75 F g^{-1} in 0.1 M K_2SO_4. Thin film Fe_3O_4 electrodes showed a SC of 170 and 25 F g^{-1} in the Na_2SO_3 and Na_2SO_4 electrolytes, respectively [21]. The highest capacitance of 510 F g^{-1} of Fe_3O_4 in a voltage window of 1.2 V was achieved for the composite Fe_3O_4-carbon black (3 wt.% Fe_3O_4) electrodes using sodium sulphite as the electrolyte [22].

4. Conclusions

In summary, Fe_2O_3 thin films have been prepared by simple and inexpensive successive ionic layer adsorption and reaction (SILAR) method. XRD pattern revealed that the Fe_2O_3 thin film exhibits amorphous nature. From scanning electron micrograph images it is seen that Fe_2O_3 film surface was well covered with irregular shaped grains. Contact angle measurement showed Fe_2O_3 surface was superhydrophilic with contact angle less than 10°. The optical studies showed direct band gap energy of 2.2 eV. The Fe_2O_3 electrode exhibited the interfacial capacitance of 0.12 F cm^{-2} and the supercapacitance of 178 F g^{-1} which is high as compared to Fe_2O_3 films. These results demonstrate that chemically deposited Fe_2O_3 thin film is a good candidate as electrode material for electrochemical capacitor.

Acknowledgement

Authors are grateful to the University Grants Commission (UGC), New Delhi for financial support through the scheme no. 36-209/2008 (SR).

References

[1] B.E. Conway, Electrochemical Supercapacitors, Scientific Fundamentals and Technological Applications, Kluwer Academic/Plenum Press, New York, 1999.
[2] D.P. Dubal, D.S. Dhawale, R.R. Salunkhe, V.J. Fulari, C.D. Lokhande, J. Alloys Compd. 497 (2010) 166.
[3] K.W. Nam, K.B. Kim, J. Electrochem. Soc. 149 (2002) 346.
[4] C. Lin, J.A. Ritter, B.N. Popov, J. Electrochem. Soc. 145 (1998) 4097.
[5] H.Y. Lee, J.B. Goodenough, J. Solid State Chem. 148 (1999) 81.
[6] D.P. Dubal, D.S. Dhawale, R.R. Salunkhe, V.S. Jamdade, C.D. Lokhande, J. Alloys Compd. 492 (2010) 26.
[7] S. Duhan, S. Devi, Int. J. Electron. Eng. 2 (2010) 89.
[8] T. Maruyama, Y. Shinyashiki, Thin Solid Films 333 (1998) 203.
[9] N. Nagarajan, I. Zhitomirsky, J. Appl. Electrochem. 36 (2006) 1399.
[10] J.D. Desai, H.M. Pathan, S.K. Min, K.D. Jung, O.S. Joo, Appl. Surf. Sci. 252 (2005) 1870.
[11] H.M. Pathan, C.D. Lokhande, Bull. Mater. Sci. 27 (2004) 85.
[12] T.P. Gujar, V.R. Shinde, C.D. Lokhande, W.Y. Kim, K.D. Jung, O.S. Joo, Electrochem. Commun. 9 (2007) 504.
[13] S. Karuppuchamy, J.M. Jeong, J. Oleo Sci. 55 (2006) 263.
[14] V.R. Shinde, C.D. Lokhande, R.S. Mane, S.H. Han, Appl. Surf. Sci. 245 (2005) 407.
[15] R.D. Sun, A. Nakajima, A. Fujushima, T. Watanabe, K. Hashimoto, J. Phys. Chem. B 105 (2001) 1984.
[16] O. Bockman, T. Ostvold, G.A. Voyiatzis, G.N. Papatheodorou, Hydrometallurgy 55 (2000) 93.
[17] R.S. Mane, J. Chang, D. Ham, B.N. Pawar, T. Ganesh, B.W. Cho, J.K. Lee, S.H. Han, Curr. Appl. Phys. 9 (2009) 87.
[18] S. Patil, M.A. More, R.B. Gore, S.V. Rao, P.P. Patil, Mater. Sci. Eng. B 65 (1999) 145.
[19] T.P. Gujar, W. Kim, I. Puspitasari, K.D. Jung, O.S. Joo, Int. J. Electrochem. Sci. 22 (2007) 666.
[20] T. Brousse, D. Belanger, Electrochem. Solid State Lett. 6 (2003) A244.
[21] S.Y. Wang, K.C. Ho, S.L. Kuo, N.L. Wu, J. Electrochem. Soc. 153 (2006) A75.
[22] N.L. Wu, S.Y. Wang, C.Y. Han, D.S. Wu, L.R. Shiue, J. Power Sources 113 (2003) 173.